MJFAS
Malaysian Journal of Fundamental and Applied Sciences

Kusumaningrum *et al.* | Malaysian Journal of Fundamental and Applied Sciences, Vol. 19 (2023) 707-721

RESEARCH ARTICLE

Synthesis of Nanomagnetite/Crosslinked Carboxymethyl *kappa* Carrageenan Nickel Imprinted Composite

Irma Kartika Kusumaningrum[a,b*], Mira Nur Fadilah[a], Anugrah Ricky Wijaya[a], Habiddin Habiddin[a], Meliza Armaya[a]

[a]Department of Chemistry, Faculty of Mathematics and Natural Sciences, Universitas Negeri Malang, Jl. Semarang 5 Malang, 65145, Indonesia; [b]Center of Advance Material and Renewable Energy, Universitas Negeri Malang (CAMRY UM) Jl. Semarang 5 Malang, 65145, Indonesia

Abstract Nickel(II) ions are carcinogenic water pollutants. To increase the accuracy of instrumental analysis of Ni(II) content, several analytical preparation methods have been developed, including solid phase adsorption extraction. The development of magnetic solid phase extraction adsorbents for metal ions is required, to support the application of magnetic solid phase adsorption as a method of separating metal ions in aqueous samples. This research describes the synthesis of Magnetic Solid Phase Extraction adsorbents as Ni(II) ion adsorbents, nano magnetite/carboxymethyl kappa-carrageenan (CMKC) crosslinked bisphenol A diglycidyl ether (BADGE) imprinted Ni(II)-IIP ion composites. This research was carried out in several stages, synthesis and characterization of nano magnetite (NM), synthesis and characterization of CMKC, and synthesis of NM/CMKCNi(II)-IIP adsorbents. The results of the synthesis were analyzed for morphological characteristics, magnetic strength, spectral characteristics, crystallinity, and composition using SEM, FTIR, XRD, and XRF instruments. The adsorption ability of Ni(II) of the adsorbent was tested. Determination of Ni(II) ion content in the sample before and after adsorption was carried out using a flame atomic absorption spectrophotometer (FAAS). Based on the results of spectral character analysis, crystal diffraction patterns, magnetic strength, and morphology, it is confirmed that nano-magnetite has been successfully synthesized. The diameter of the nano magnetite grains is 21.8 nm, the adsorbent NM/CMKCNi(II)-IIP has magnetic properties and wavy surface morphology. The optimum adsorption ability of Ni(II) for the NM/CMKCNi(II)-IIP composite was 2.44 mg Ni(II)/g adsorbent. To evaluate the tendency of the adsorption ability of the adsorbent towards Ni(II) ions in the presence of competitor ions, the adsorption ability of the adsorbent to adsorp Ni(II) ions in samples containing Ni(II) ions, Pb(II) ions and a mixture of Ni(II) ions. and Pb(II) were determined, based on the results of the analysis, the ability of the adsorbent to adsorb Ni(II) ions was higher than the ability of the adsorbent to adsorb Pb(II) ions, in all types of samples.

Keywords: Nano magnetite, Adsorption, NM/CMKCNi(II)-IIP, Carboxymethyl k-Carrageenan, Ni(II) ion.

***For correspondence:**
Irma.kartika.fmipa@um.ac.id

Received: 19 May 2023
Accepted: 22 August 2023

Introduction

Nickel(II) ion is a carcinogenic water pollutant [1]. Developing an analytical method for determining the content of Nickel(II) in water to improve the accuracy of the analysis results is one of the interesting studies. Difficulties are often found in the analysis of metal ion levels in water if the metal ion content is very low or the composition of the sample is complex, selective ion adsorption methods and solid phase adsorption are often used to increase the concentration of metal ions in samples and remove non target ions [2]. Today, magnetic solid phase extraction has been developed to separate metal ions in a mixture by adsorbing metal ions on the surface of the adsorbent in the form of modified nano magnetite and then attracting the adsorbent using an external magnetic field. The advantages of magnetic solid phase

extraction are (1) faster procedures, (2) easy analyte separation, (3) easy recycle and reuse [3]. Magnetic solid phase extraction (MSPE) has been used to separate metal ions in mixtures [4]. The surface of the magnetic adsorbent absorbs metal ions in the mixture and then the adsorbent is localized and pulled out of the sample vessel directed by an external magnetic field. MSPE has been widely applied in several fields, such as biomedical [5]; [6], environmental science [7]; [8], forensic science [9] and food analysis [10]; [11]. The advantages of the MSPE technique are speed and ease in separating the adsorbent material from the sample matrix [4].

MSPE adsorbent, a magnetic composite consisting of magnetic parts, and other composite materials that carry out certain functions. The function of magnetic composites is engineered through modification of composite materials. The MSPE principle is to bind the analyte in the sample solution to the surface of the magnetic adsorbent, then the adsorbent is separated from the sample solution by the attraction of an external magnetic field. The analyte is then eluted from the adsorbent with a suitable solvent, so that the eluate containing analyte is ready to analyzed [12]. The most commonly used magnetic material is nano magnetite (Fe_3O_4), which has superparamagnetic properties [13]. Nanomagnetism combined with various coatings or composite materials, designed to adsorb metal ions which can then be desorbed again using a desorption solvent [14].

The previous researchers has developed the use of nano magnetite/carboxymethyl *k*-carrageenan(CMKC) composite as an adsorbent for Cr(III), Cu(II), Ni(II) and Co(II) metal ions[15], biomaterial adsorbent [16], metal ion preconcentration media in samples containing single ions Cu(II), Co(II), Ni(II) and Cr(II) [17], a mixture of metal ions Ni(II) and Cr(III) [18], a mixture of Pb(II) and Cu(II) [19]. Some previous research results show that nano magnetite/CMKC can adsorb various metals simultaneously.

Adsorption of metal ions on the nano magnetite/CMKC surface is likely due to the interaction between CMKC carbonyl anionic groups with cationic metal ions, and polymer pore entrapment. CMKC polymer can swell so that the size of the gaps between polymer chains increases during the swelling process, so that metal ions become difficult to be trapped into the pores, and then the ability of the polymer as an adsorbent decreases. Attempts to develop reusable nano magnetite-based adsorbents requires an adsorbent with stable adsorption capacity. Nano magnetite/CMKC has been used as an adsorbent for metal ions; their adsorption capacity reaches 99.72% for Ni(II) ions [20] and 0.1 g Pb^{2+}/ 1 g Nano magnetite/CMKC [21]. Unfortunately, CMKC has a high swelling ability [22]. So that the adsorption ability of nano magnetite/CMKC decreases when exposed to contact for a long time or repeated use in aqueous media [23].

Various techniques carry out polymer modification. The crosslinking technique strengthens the polymer structure due to the formation of bonds that link between polymer chains [24]. Cross linking also allows the formation of a pattern of polymer chain arrangement. The printed polymer technique produces polymers with specific templates, which are recognized by the ion/similar molecules contacted after ion imprinting [25]. [26] carried out cross-linking of carboxymethyl chitosan with bisphenol A diglycidyl ether (BADGE); this cross-linking brought the carboxymethyl chitosan carbonyl groups closer together which allowed the carbonyl lone pair to form a covalent bond to bind to the Pb(II) metal ion. The binding of metal ions is followed by the release of Pb(II) ions which are bound to the polymer, resulting in the formation of gaps printed by Pb(II) ions, on polymers. Imprinting ion holes on the polymer surface produces ion imprinted polymer (IIP) which have specific receptor sites for target ions [27]. This technique can be used to make selective adsorbents. Polymer cross-linking also increases the mechanical strength of the polymer. CMKC is a biopolymer that is able to adsorb metal ions, but CMKC's swelling power is high, so its adsorption ability decreases and its morphology is damaged when it is reused. Crosslinking is an alternative to increase mechanical strength and reduce swelling. Crosslinking also affects the process of ion mold formation. This method has not been studied for CMKC. This article presents the results of a research on the synthesis of nano magnetite/carboxymethyl *kappa*-carrageenan adsorbents cross-linked with bisphenol A diglycidyl ether (BADGE), Ni(II) ion imprinted as Ni(II) ion adsorbents.

Materials and Methods

Apparatus

Apparatus used: FTIR (Prestige 21 Shimadzu), SEM (FEI, Type: Inspect-S50), Flame-Atomic Absorption Spectrophotometer (AAS), XRD (AAP analytical, Type: Expert Pro), XRF (PANalytical, Minipal 4), ovens (Memmert), shaker, universal indicators, filter paper, standart laboratory equipment and glassware.

Material

The material used: kappa-carrageenan powder (food grade, local market), NaOH p.a, 96% ethanol, isopropyl alcohol (IPA), glacial acetic acid, nitric acid, monochloroacetic acid (MCA), bisphenol A Diglycidyl Ether (BADGE) p.a, HCl p.a 37%, distilled water, aqua demineralization, $FeCl_3.4H_2O$ p.a, $FeSO_4.4H_2O$ p.a, $NiCl_2.6H_2O$ p.a and $Pb(NO_3)_2$ p.a. All reagents from Merck.

Nanomagnetite Synthesis

A mixture of 25 mL of 0.125 M $FeSO_4.7H_2O$ solution and 0.25 M $FeCl_3.6H_2O$ solution (1:1 v/v) was added dropwise into 50 mL of 0.5 M NaOH while stirring using a magnetic stirrer for 30 minutes. The black residue obtained was filtered using fine filter paper, then neutralized using distilled water, dried in an oven at 50-60°C for 5 hours, then sieved through a 100 mesh sieve. The synthesized nano magnetite powder was characterized using SEM, FTIR, VSM and XRD instruments.

CMKC Synthesis

One gram of *k*-carrageenan was suspended in 25 mL of isopropanol, the suspension was stirred at room temperature for 15 minutes, 3 mL of ethanol was added, then stirred for 10 minutes. The suspension was added 2.4 grams of NaOH 3 times every 15 minutes, after stirring at 70°C for 1 hour, and a solution of 2.5 grams of MCA was added in 10 mL of ethanol while still being heated at 50-60°C for 4 hours. The suspension was then filtered, and the residues obtained were suspended in 10 mL ethanol, and neutralized with a glacial acetic acid solute. The suspensions were filtered using filter paper, and their residues were washed with 10 mL ethanol until the washing water was neutral. The residue CMKC was then dried at 60°C for 24 hours. CMKC were characterized using FTIR instrument.

Synthesis of Nanomagnetite/bisphenol a Diglisidil eter (BADGE) Crosslinked Ni (II) Imprinted Composite (NM/CMKCNi(II)IIP) and Nanomagnetite/bisphenol a Diglisidil Eter (BADGE) Crosslinked CMKC Composite (NM/CMKCNi(II))

One gram of nanomagnetite and 4 grams of CMKC were suspended in 100 mL of aqua DM, and stirred for 1 hour at room temperature. Then the mixture was added to a glass flask containing 500 mL of 0.02 M $NiCl_2$ solution and stirred for 20 hours to adsorb Ni(II) ions. The product formed is a NM/CMKCNi(II) composite. The NM/CMKCNi(II) obtained was put into a round flask containing 150 mL of distilled water, 5 mL of 1 M NaOH, and 4.029 g of bisphenol A diglycidyl ether (BADGE), refluxed for 6 hours. The product is filtered, washed with ethanol and distilled water until the pH is neutral. The product formed is NM/CMKCNi(II)-BADGE. The release of Ni(II) process from NM/CMKCNi(II)-BADGE was carried out by soaking NM/CMKCNi(II)-BADGE in 50 mL 0.1 M HCl solution for 4 hours, then filtered and washed repeatedly with 0.1 M HCl, 50 mL/each repetition the washing filtrat is dripped with NaOH 2 M until the pH of the filtrat is > 9, dimethyl glyoxim solution (DMG) 0,001 M dripped onto the washing filtrate, if a red precipitate is still formed in the filtrate after DMG is dropped, the adsorbent is washed again with HCl, the process is repeated until no red precipitate forms when DMG is dropped, the last adsorbent washing filtrate was stored and tested for Ni(II) ion content with AAS. Then the adsorbent was washed with distilled water until neutral and dried in an oven at 60°C for 48 hours. The final product is a nano magnetite/BADGE cross-linked CMKC Ni(II) imprinted composite (NM/CMKCNi(II)IIP) was characterized by VSM, FTIR, SEM and XRF. Synthesis of (NM/CMKCNi(II)) carried out with the same method as the synthesis method of NM/CMKCNi(II)IIP without the leaching process of NM/CMKCNi(II)-BADGE.

Synthesis of Nanomagnetite/CMKC Composite

One gram of nano magnetite and 4 grams of CMKC were suspended in 100 mL of aqua DM, stirred for 20 hours at room temperature. The product formed is a NM/CMKC composite. The NM/CMKC obtained soaked in 0.1 M HCl solution for 4 hours, filtered, and repeatedly washed with aqua DM until the wash water was neutral and then dried in an oven at 60°C for 48 hours. The final product is NM/CMKC composite characterized using FTIR and SEM Instrument.

.

Synthesis of Nanomagnetite/bisphenol a Diglisidil Eter (BADGE) Crosslinked CMKC Composite (NM/CMKCBADGE)

Nano magnetite/BADGE cross-linked CMKC composite non ion imprinted was synthesized as a comparison material. One gram of nano magnetite and 4 grams of CMKC were suspended in 100 mL of aqua DM, stirred for 20 hours at room temperature. The product formed is a NM/CMKC composite. The NM/CMKC obtained was put into a round flask containing 150 mL of distilled water, 5 mL of 1 M NaOH and 4.029 g of bisphenol A diglycidyl ether (BADGE), refluxed for 6 hours. The product is filtered, washed with ethanol and distilled water until the pH is neutral. The product formed is NM/CMKCBADGE.

NM/CMKCBADGE was soaked in 0.1 M HCl solution for 4 hours, filtered, and repeatedly washed with aqua DM until the wash water was neutral and then dried in an oven at 60°C for 48 hours. The final product, BADGE cross-linked NM/CMKC composite, was characterized using FTIR, SEM and XRF instrument.

Adsorption Capacity Test of NM/CMKCNi(II)-IIP as Ni(II) Metal Adsorbent

Prepared two part of each 40 mL of sample solution containing 1 ppm of Ni(II) ions in two different Erlenmeyer. After that, 15 mg of NM/CMKCNi(II)-IIP adsorbent was added to Erlenmeyer A and 15 mg of NM/CMKC-BADGE (NIP) adsorbent to Erlenmeyer B. Shaken with a shaker for 40 minutes at room temperature, then the adsorbent was withdrawn with an external magnetic field and the content of Ni(II) contained in the adsorbate is determined by SSA. Repeat these steps by changing the adsorbent mass to 5; 7.5; 20; and 30 mg to determine the maximal adsorption capacity. The adsorption capacity was determined by means of graphical analysis of plots of % Ni(II) adsorbed against the mass of the adsorbent, at the optimal point of adsorption. Adsorption selectivity was analyzed based on a comparison of the adsorption ability of NM/CMKCNi(II)IIP as adsorbent Ni(II), Pb(II) in sample solutions Ni(II), Pb(II) and a mixture of Ni(II)-Pb(II), a test carried out at a concentration of Ni(II) close to the adsorption capacity of the adsorbent on Ni(II) which was determined in the experiment to determine the adsorption capacity of NM/CMKCNi(II)IIP previously.

Results and Discussion

Synthesis and Characterization of Nanomagnetite (Fe_3O_4)

Magnetite material Fe_3O_4 has been synthesised by the coprecipitation method. A mixture of $FeSO_4.7H_2O$ solution and $FeCl_3.6H_2O$ solution was reacted with NaOH solution, so the following reaction occurred.

$$Fe^{2+}(aq) + 2Fe^{3+}(aq) + 8OH^{-}(aq) \rightarrow Fe_3O_4(s) + 4H_2O(l) \quad (1)$$

The synthesis result in a solid black material that is attracted by an external magnet. The physicochemical character of the synthesis result was characterized by the morphology (SEM image), FTIR spectral characteristic (FTIR), and crystallinity (XRD) of the synthesis result. The results of the FTIR analysis in Figure 1 shows that there are absorption peaks at wave numbers 569 cm^{-1} and 640 cm^{-1} indicating the presence of Fe-O vibrations from ferrous oxide, 631 cm^{-1} and 639 cm^{-1} [28]; [29]; [30]. There are peaks at wave numbers 3435 cm^{-1} and 1634 cm^{-1} which correlate with the stretching and bending O-H bonds, as the results of nano magnetite characterization reported by previous researchers [28]; [29]; [30], O-H bending and stretching nano magnetite vibrations appear at 1621 cm^{-1}, 1628 cm^{-1}, 1631 cm^{-1}, 3408 cm^{-1}, 3423 cm^{-1} and 3431 cm^{-1}.

The XRD diffractogram pattern for a type of compound crystal is typical, each compound crystal has a different pattern. Therefore the XRD diffractogram pattern is used to identify the type of compound. Based on JCPDS database No 19-0629 (Joint Committee For Powder Diffraction Standard), the peaks of the nano magnetite XRD diffractogram measured at an angle of 2θ are 18.2°, 30.1°, 35.4°, 37.1°, 53.4°, 56.9°, 62.5°, 65.7°, 70.9°, 73.9°. Figure 2 shows the synthesized XRD diffractogram measured at an angle of 2θ with peaks at 29.93°, 35.43°, 43.40°, 57.41°, and 62.74°. The synthesized XRD diffraction peaks showed close to the magnetite diffractogram peaks in the JCPDS database. Previous researchers stated that the magnetite XRD diffractogram have peaks at 30.31°, 35.92°, 43.6°, 57.38°, and 62.96° [31]. The other researchers also stated that the peaks of magnetite XRD pattern are 18.01° , 30.284° , 35.662°, 43.289°, 53.5° , 57.173° , 62.844°, 71.351° , and 74.284° [32]. Based on the XRD diffractogram pattern synthesized which is close to the peak pattern of the JCPDS diffractogram and the XRD diffractogram pattern of previous researchers who have characterized magnetite, it can be concluded that the synthesized material is magnetite.

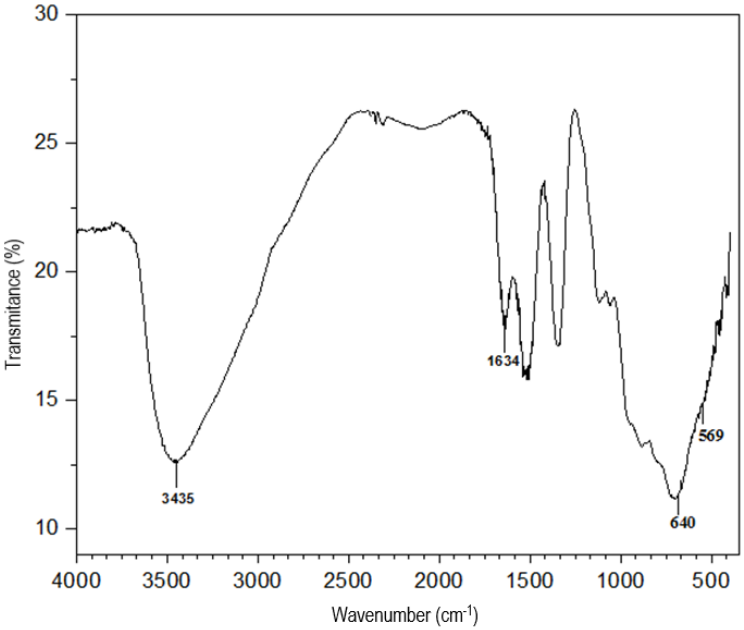

Figure 1. FTIR Spectrum of Nanomagnetite (Fe_3O_4)

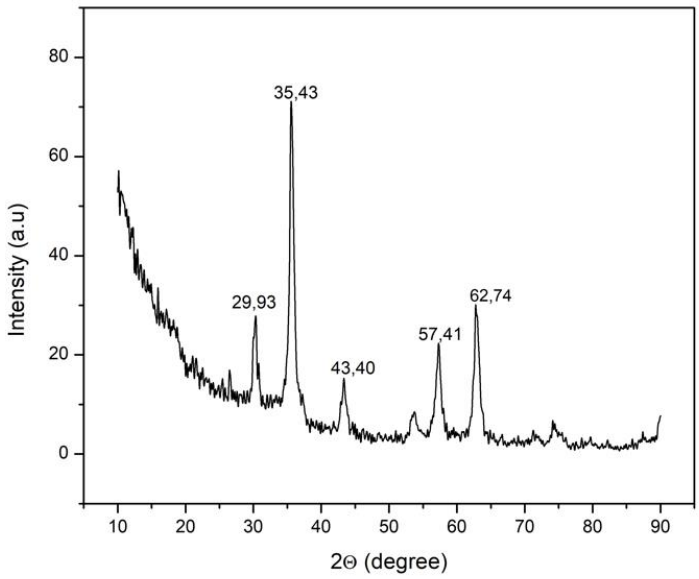

Figure 2. Diffractogram of synthesized nanomagnetic (Fe_3O_4)

Based on the results of XRD analysis, the size of nano magnetite crystals can be determined by the Scherrer equation as follows:

$$D = \frac{k\,\lambda}{\beta \cos\theta} \tag{2}$$

Equation (2) calculates the average particle diameter of 21.8 nm. The Scanning Electron Microscope (SEM) is used to analyse the morphology of the magnetite synthesised material, Figure 3(a) is an SEM image of the magnetite material at 50,000x magnification.

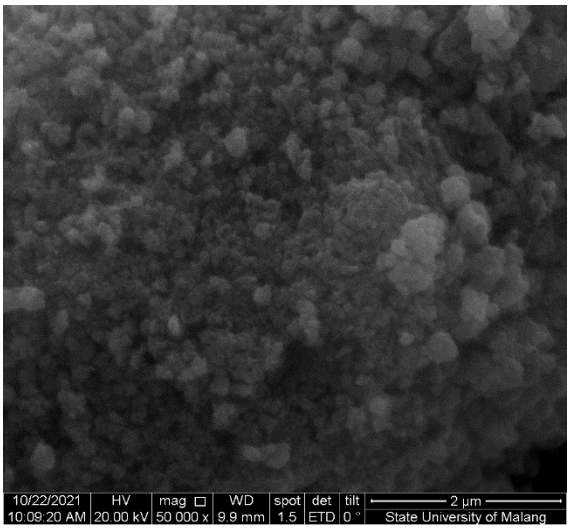

Figure 3. Morphology of Nanomagnetite (Fe_3O_4)

Magnetism was studied using the VSM instrument, obtaining hysteresis curve data [33]. The hysteresis curve shows the relationship between the magnetisation (M) and the external magnetic field (H). Based on Figure 4, it appears that the area of the hysteresis curve is narrow, indicating that the synthesised nano magnetite (Fe_3O_4) is a soft magnet. The magnet saturation value is M 56.92 emu/gr, while the coercivity field value is 0.01174 (KOe), shows that the synthesized nano magnetite is a weak magnet, the remanent magnetization value is 3.66 emu/gr. This magnetic force can attract the paramagnetic metal ions, leading to a magnetic adsorbent. When the magnetic force acts on the paramagnetic metal ion, there will be an increase in the intensity of the magnetic field which attracts the ion towards the center of the field [34]. Nickel will be pulled towards the composite adsorbent by the magnetic components contained in the adsorbent.

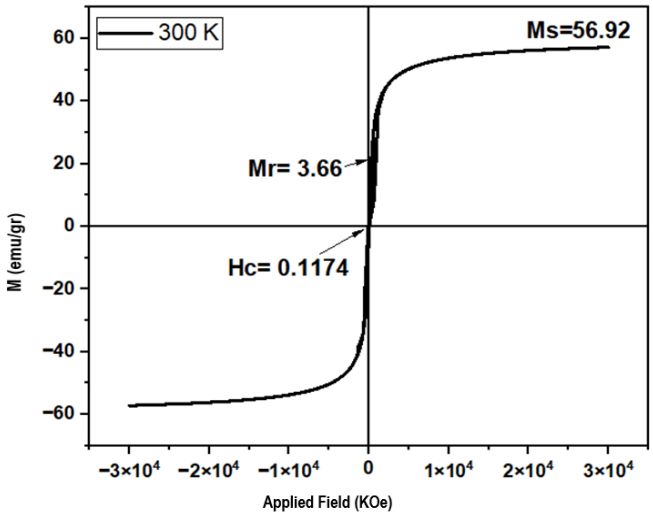

Figure 4. Hysteresis Curve of Nanomagnetite (Fe_3O_4)

Synthesis and Characterization of Carboxymethyl Kappa-carrageenan (CMKC)

Carboxymethyl *k*-carrageenan (CMKC) is a *kappa*-carrageenan derivative made by carboxymethylation of the hydroxyl groups on the *k*-carrageenan polymer chain, *k*-carrageenan is reacted with NaOH, to produce alkoxy *k*-carrageenan which is then reacted with monochloroacetic acid (MCA), follow the reaction in Figure 5.

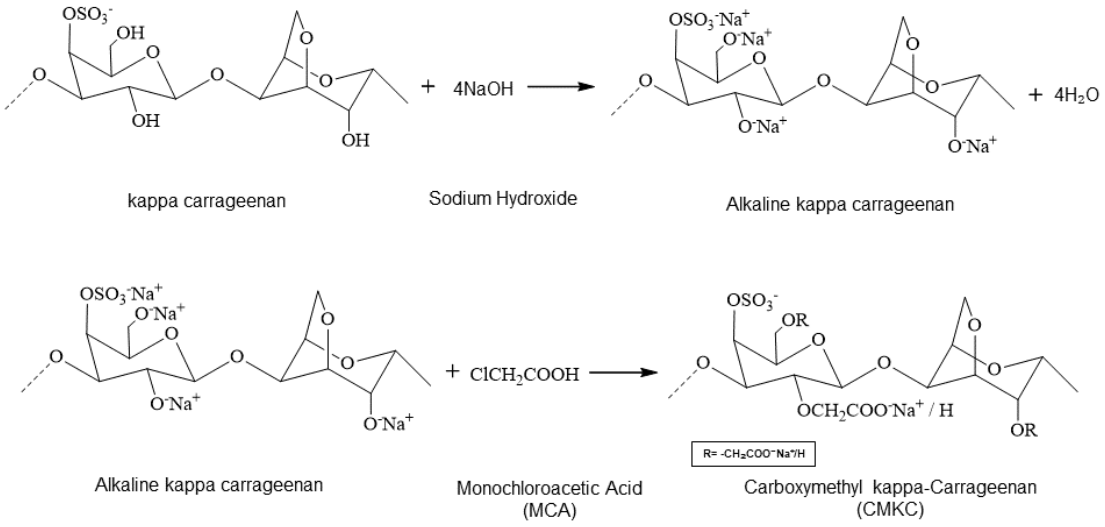

Figure 5. Steps of Alkalization reaction (a) and Etherification reaction (b)

The conversion of the k-carrageenan hydroxyl group to a carboxyl group causes a change in the FTIR spectrum. The difference in the FTIR spectra of *k*-carrageenan and CMKC can be seen in Figure 6. The main absorption bands of *k*-carrageenan and CMKC and their correlation with functional groups are presented in Table 1. Typical absorption bands of *k*-carrageenan appear at wave numbers 1278 cm^{-1} and 844 cm^{-1} indicating a symmetrical O=S=O vibration and a C-O-S stretching vibration. The absorption band at wave number 931 cm^{-1} shows C-O-C from the 3,6-anhydrogalactose group. The absorption band at wave number 1077 cm^{-1} and widening of the absorption band at 2915 cm^{-1} indicate C-O strain and C-H strain. The carboxymethylation reaction converts the hydroxyl group on *k*-carrageenan to a carboxyl group.

The CMKC FTIR spectrum shows absorption bands at wave numbers 1604 cm^{-1} and 1443 cm^{-1} correlated with the strain of the carboxylate anion (-COO-), besides that absorption bands, appear at wave numbers 1773.12 cm^{-1} indicating the presence of stretching vibrations on the carbonyl group. The absorption band shift occurred in the –OH group absorption band, in *k*-carrageenan it was seen at wave number 3480 cm^{-1} while in CMKC it appeared at 3447 cm^{-1}, indicating that some of the -OH groups in *k*-carrageenan had been converted.

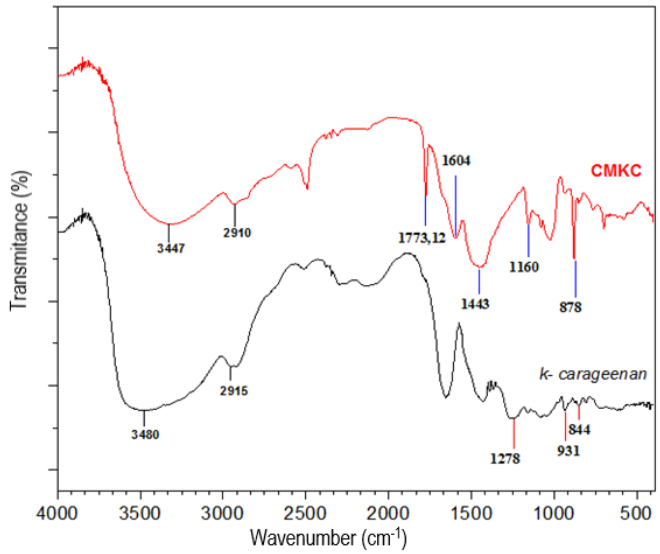

Figure 6. FTIR spectrum of CMKC and *k*-Carrageenan

Table 1. FTIR Spectrum Peak Correlation on *k*-Carrageenan and CMKC

Functional groups	Wave Number (cm^{-1})		Reference	
	Kappa-Carrageenan	CMKC		
O-H	3480	3447	3300 cm^{-1}[35][35][35]	[36]
C-H	2915	2910	2929 cm^{-1}[35][35][35]	[36]
C=O	-	1772,58	1746 cm^{-1}	[37]
COO^-	-	1604; 1443	1597 cm^{-1}; 1424 cm^{-1}	[16]
O=S=O	1278	-	1224-1228 cm^{-1}	[16]
C-O	1078	1077	1024 cm^{-1}	[38]
C-O-C	931	-	925-928 cm^{-1}	[16]
C–O–S	844	878	850 cm^{-1}	[16]

Synthesis and Characterization of NM/CMKCNi(II)IIP

The adsorbent, NM/CMKCNi(II)IIP composite was synthesised in several steps. In the first step CMKC and nanomagnets were suspended in distilled water, nanomagnetite is bound to CMKC through the interaction between Fe^{2+}/Fe^{3+} with O- from the hydroxyl group, binding of nanomagnetite through the interaction between Fe^{2+}/Fe^{3+} nanomagnetite and hydroxyl groups has been described by other researchers [39]. Figure 7 illustrates the bonding between NM and CMKC

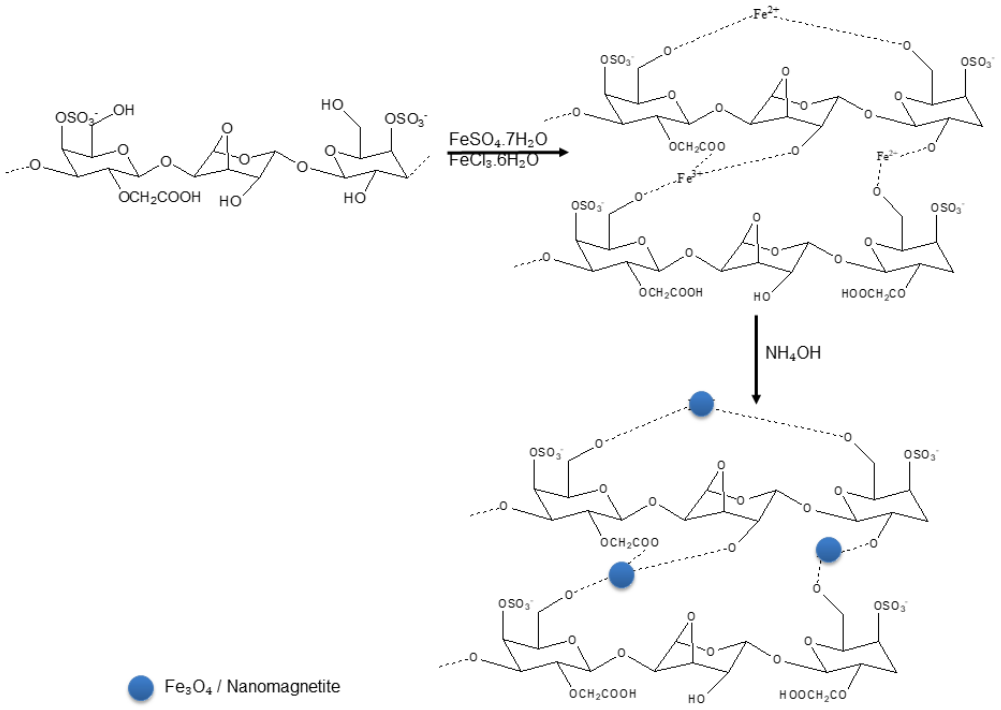

Figure 7. The bonding between NM and CMKC

Ni(II) ions were bound to produce NMCMKCNi(II), Ni(II) is bound by the CMKC carboxyl group, the product was crosslinked with bisphenol A diglycidyl ether (BADGE). Cross-linking causes the polymer chains to closer each other compared to the uncross-linked polymer [3]. This position allows the free electrons of the carbonyl groups of the CMKC polymer chains interact with metal ions that have been bound by the carbonyl groups of the other CMKC polymer chains, as shown in Figure 7. The third step

was the release of Ni(II) ions. The ion release process is a step to form a hole according to the ion printer. The holes selectively bind to the same metal ions as the printer ions. The resulting product is a composite NM/CMKCNi(II)IIP which is attracted by a magnet. Nanomagnetite is bound to CMKC through the interaction between Fe^{2+}/Fe^{3+} with O^- from the hydroxyl group. Figure 8 illustrates the synthesis scheme of the NM/CMKCNi(II)IIP adsorbent through several steps. CMKC, which has bound Ni(II), was cross-linked with BADGE, this binding model has been proposed by previous researchers, who conducted cross-linking experiments of carboxymethyl cellulose polymers with BADGE [26]. The CMKC cross-linking reaction in this study proceeded as the reaction is shown in Figure 9.

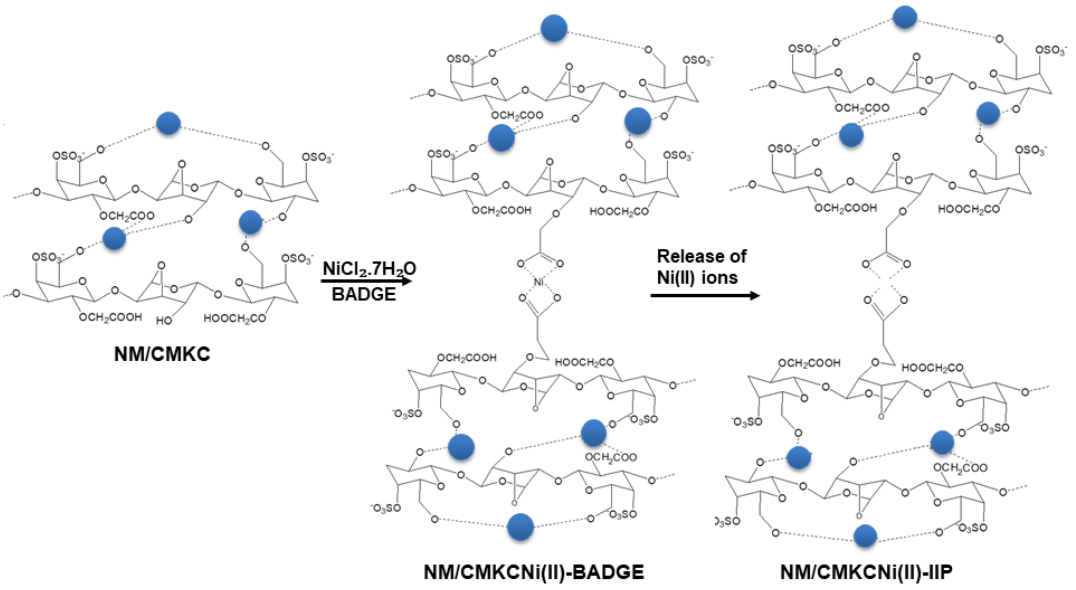

Figure 8. Synthesis scheme of the NM/CMKCNI(II)IIP adsorbent

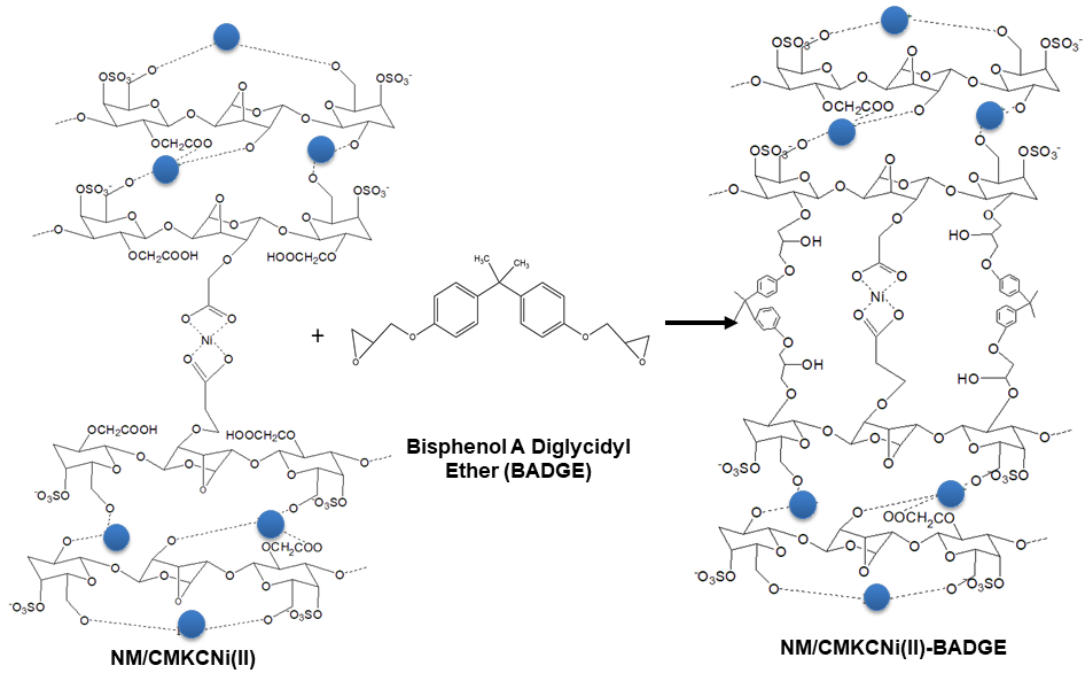

Figure 9. Crosslinking reaction of NM/CMKCNi(II) with BADGE

The FTIR spectrum of the CMKC, NM/CMKC composite (Figure 9) shows that the crosslinking, metal ion binding and ion releasing processes cause the CMKC's carboxyl group absorption band wave number shift. The asymmetric –COO absorption band of the CMKC carboxyl group of the nano magnetite-CMKC composite (NM/CMKC) appears at wave number 1644 cm^{-1}, whereas the –COO's bands peak of the uncrosslinked NM/CMKC composite which binds Ni(II) appears at wave number 1615 cm^{-1}, the asymmetric –COO's absorption band of the cross-linked NM/CMKC composite that binds Ni(II) (NM/CMKCNi(II)) appears at 1638 cm^{-1} and after Ni(II) ion was released, the asymmetric –COO absorption band of (NM/CMKCNi(II))IIP appears at 1625 cm^{-1}, the wave number shift of the absorption band correlates with the changes of the carboxyl group bond's rigidity.

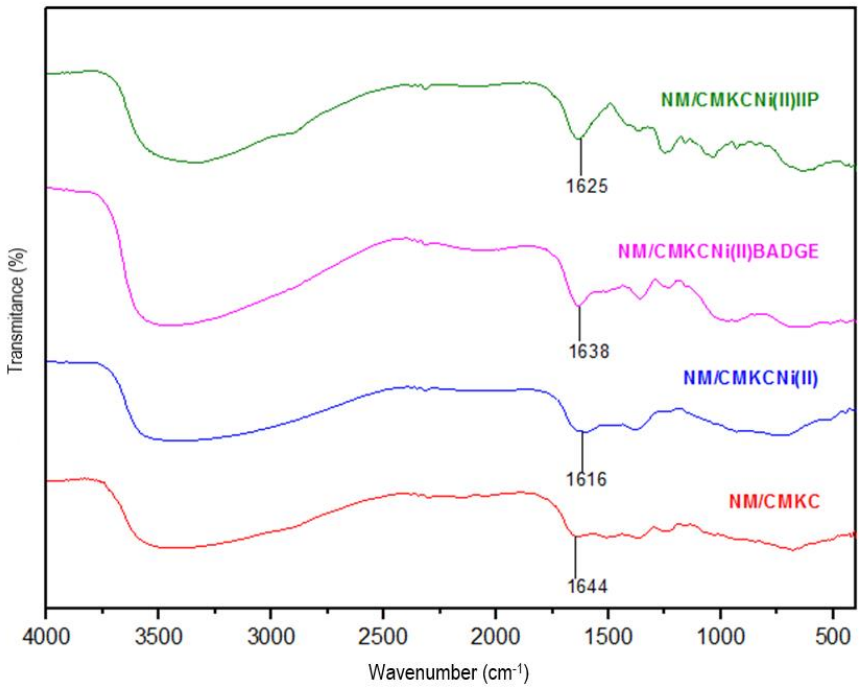

Figure 10. FTIR spectrum of NM/CMKCNi(II)IIP, NM/CMKCNi(II)BADGE, NM/CMKCNi(II) and NM/CMKC Composites

The interaction between the CMKC's carboxyl group with Ni(II) reduces the electron density in –COO group of NM/CMKC, because the electrons are attracted towards Ni(II), so the energy for vibrational absorption decreases. The –COO absorption peak's wave number of NM/CMKC is higher than the –COO absoption peak's wave number of NM/CMKMNi(II) that has the lower electron density. NM/CMKCNi(II) cross-linking causes an increase in the rigidity of the structure around the carboxyl group due to the attraction of the cross-links, because of that the vibrational energy of –COO on NM/CMKCNi(II) is higher than that of NM/CMKC, so that the absorption band shifts to a lower wave number, higher. The release of metal ions from NM/CMKCNi(II) causes the rigidity of the structure to decrease, because the metal ions bridging the two polymer chains are released, the vibrational energy decreases, therefore the –COO vibrational energy on NM/CMKCNi(II)IIP is lower than the –COO vibrational energy NM/CMKCNi(II), –COO NM/CMKCNi(II)IIP absorption band appears at a lower wave number than the -COO NM/CMKCNi(II) absorption band.

The synthesis process of the NM/CMKCNi(II)IIP adsorbent was preceded by the synthesis of NM/CMKCNi(II)-Badge, Ni(II) ions were released from NM/CMKCNi(II)-Badge, then the NM/CMKCNi(II)IIP was resulted. XRF analysis data were used to analyze the quantity of Ni(II) ions bound to the surface of NM/CMKCNi(II)-Badge and Ni(II) remaining on the surface of NM/CMKCNi(II)IIP after the Ni(II) ions as an ion mold former were leached from NM/CMKCNi(II)-Badge. The nickel percentage of NM/CMKCNi(II)-Badge, is 15.3%, indicating that a certain amount of nickel is bound to NM/CMKCNi(II)-Badge, after the leaching process, the nickel percentage of NM/CMKCNi(II)-Badge decreases to 0.95%. Table 2 show the percentage of the NM/CMKCNi(II)-Badge and the NM/CMKCNi(II)IIP.

The nickel concentration of leaching process's washing filtrate was determined using AAS to monitor the reduction of Ni(II) present in NM/CMKCNi(II)-Badge which is being leached. Table 3 show the nickel concentration of the washing filtrate.

Characterization using SEM is used to see the surface morphology of the composite. The morphology of the NM/CMKCNi(II) composite without crosslinking, the NM/CMKCNi(II)-Badge composite before the release of Ni(II) ions, and the composite after the process of releasing metal ions or called NM/CMKCNi(II)IIP is shown in Figure 10.

Table 2. Percentage of NM/CMKCNi(II)-Badge and the NM/CMKCNi(II)IIP

Metal Elements	NM/CMKCNi(II)-Badge	NM/CMKCNi(II)IIP
Ca	0,76%	0,26%
Ti	0,49%	0,53%
V	0,02%	0,03%
Cr	0,16%	0,22%
Mn	0,26%	0,34%
Fe	80,47%	92,30%
Ni	**15,30%**	**0,95%**
Br	0,35%	0,39%

Table 3. Nickel Concentration of Leaching Process's Washing Filtrate

Washing process	Nickel concentration (ppm)
1st washing	16,57
2nd washing	8,75
3rdwashing	2,20
4th washing	1,01
water	0,09

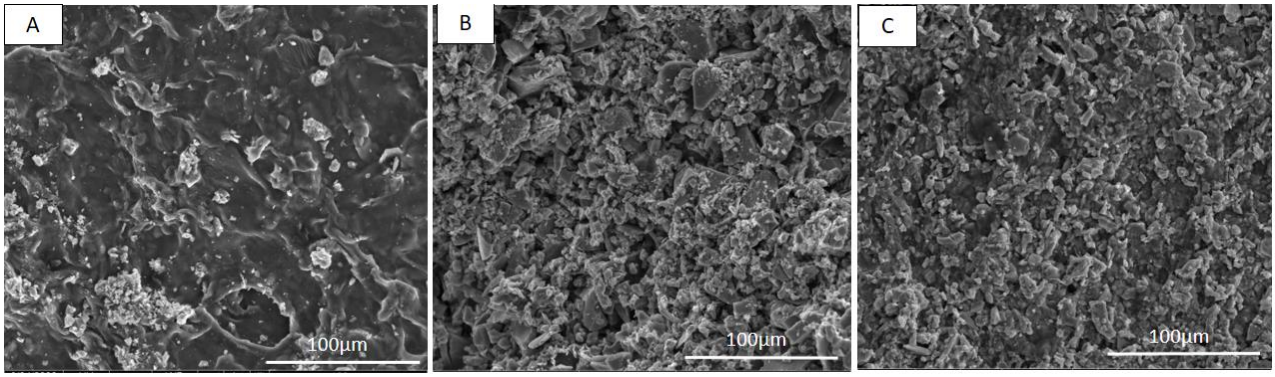

Figure 11. Surface Morphology of NM/CMKCNi(II) (a), NM/CMKCNi(II)Badge (b), NM/CMKCNi(II)-IIP (c)

Figure 11(a) shows the surface morphology of the NM/CMKCNi(II) composite, the surface folds of the nanomagnetic-CMKC composite bound to Ni(II) without crosslinking have larger waves than the NM/CMKCNi(II)-Badge composite (Figure 11b) and Crosslinked NM/CMKCNi(II)IIP (Figure 10c). When

contacted with the dispersing medium, the polymer in the composite swell, the non-crosslinked polymer swell more than the crosslinked polymer, therefore the folding wave on the non-crosslinked NM/CMKCNi(II) composite surface is larger than the polymer folding wave. The morphology of the cross-linked polymer composites shows that, in addition to the folds that occur due to the swelling process, the cross-links cause the distance between the polymer chains at the point of the cross-link knot to be smaller compared to the other parts, so that the distance between the polymer chains is tighter and knots are formed at several points. Cross-linking increases the mechanical resistance of the material, changes the morphology and porosity of the material [40]. Figure 11 (c) shows the morphology of NM/CMKCNi(II)IIP adsorbent surface, folding occurs due to swelling and crosslinking processes, as in NM/CMKCNi(II)Badge, but the folding in NM/CMKCNi(II)IIP is more small, because after the release of Ni(II) ions from the cross-linked CMKC, the bond tension of the carboxyl groups that originally bound the Ni(II) is reduced and the polymer is folded.

NM/CMKCNi(II)IIP adsorbents are designed to bind Ni(II) specifically through ion template adsorption.NM/CMKCNi(II)IIP can adsorb Ni(II) ions more selectively than Pb(II), this might happen because geometrically there has been a unique arrangement of the ligand groups to coordinate with Ni(II) ions, when Ni(II) ions interact with carboxyl groups involving the d^8 orbital, while Pb(II) has a completely filled d orbital and an incomplete p orbital. Thus printing adsorbent can cause adsorption selectivity leading to Ni(II) binding. Previous researchers stated that this explanation was to explain the selectivity of IIP adsorbents for Co(II). Non-ion imprinted binding sites can also be formed during IIP imprinting, the free carboxyl and hydroxyl groups have almost the same tendency to bind various metal ions, resulting in non-selective binding [41]. Non-specific adsorption can also occur due to pore adsorption, pores are formed when CMKC swelling.

Analysis of the adsorption ability of Ni(II) was carried out to determine the ability of the adsorbent to bind the targeted adsorbate and other metal ions. Adsorption ability is calculated through the calculation formula as follows.

$$\text{Adsorption ability}(\text{mg}/g) = \frac{\text{Adsorbed Concentration (mg/L)}}{\text{Adsorbent mass (g)}} \times V\ (L) \qquad (3)$$

The adsorption ability for Ni(II) was determined by adsorption of a sample solution of Ni(II) with a constant concentration and the amount of adsorbent increased. The adsorption ability was determined when the adsorption percentage stagnated on the addition of the adsorbent. The maximum adsorption percentage of NM/CMKCNi(II)-IIP adsorbent on Ni(II) metal ions was 89.6%, with the adsorption ability of Ni(II) adsorbent being 2.44 mg Ni(II)/g adsorbent. As a comparison material, an adsorption ability test was carried out using a comparison material NM/CMKC-Badge (Non Imprinted Polymer / NIP) at the same adsorbent mass, the percentage of NIP adsorption to Ni(II) ions was 49.89% and NIP adsorption ability to Ni ions (II) is 1.65 mg/g.

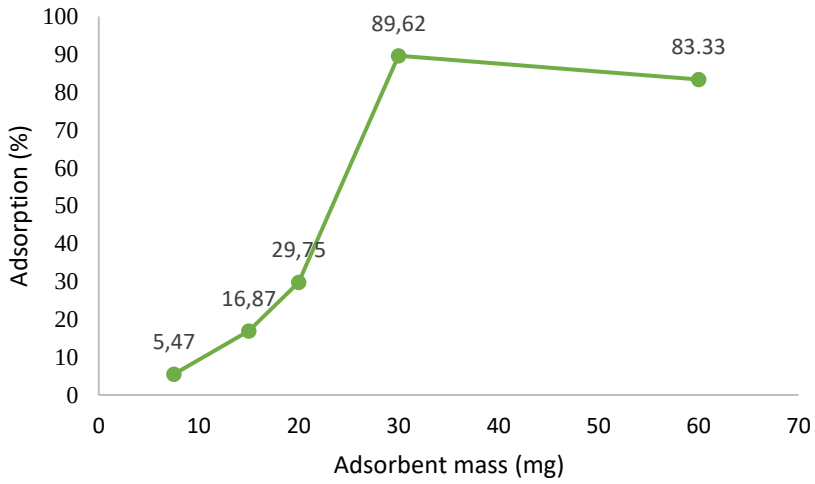

Figure 12. NM/CMKCPb(II)-IIP Percent Adsorption Ability Curve

The selectivity of the NM/CMKCNi(II)IIP adsorbents was tested by measuring the ability of the adsorbents to bind Ni(II) and Pb(II) in samples which were a mixture of Ni(II) and Pb(II) dissolved in water. The results of the experiment are shown in the Table 4.

Table 4. Test result of NM/CMKCNi(II)IIP as Ni(II) and Pb(II) adsorbent

Before Adsorption Process		After Adsorption Process				Adsorbent Mass (mg)	Kads NiII]	Kads [Pb]
[Ni(II)] ppm	[Pb(II)] ppm	[Ni(II)] ppm	[Pb(II)] ppm	% Ni(II) Adsorbed	% Pb(II) Adsorbed			
2,2802	0	1,1402	0	49,99	0	500	2,280	0
0	1,8760	0	1,6105	0	14,15	500	0	0,531
1,8300	1,9217	1,9260	1,6075	90,40	16,35	500	1,808	0,628

NM/CMKCNi(II)IIP adsorbents bind more Ni(II) than Pb(II). Pb(II) binds to an adsorbent designed to selectively bind Ni(II). It is suspected that the adsorption of metal ions on the adsorbent occurs due to ion trapping and adsorption by the gaps between the polymer chains, when the adsorbent polymer swell contact with water. The hydrated ionic radius of Pb(II) is lower than that of Ni(II), the values of hydrated ionic radius are 0.40 ˚A for Pb(II) , and 0.63 ˚A for Ni(II).The smaller the hydrated ionic radius the greater will be the affinity to penetrate into smaller pores , this was also explained by previous researchers [42].

Conclusions

Nanomagnetite (NM), CMKC, and Ni(II)/nanomagnetite, (NM/CMKCNi(II)IIP) cross-linked CMKC composites have been synthesized. The adsorbent in the form of a cross-linked kappa-carrageenan (CMKC) composite and imprinted Ni(II)/nanomagnetite (NM/CMKCNi(II)IIP) ion has magnetic characters and wavy surface morphology, the beads diameter is 21.8 nm. The adsorption capacity of the NM/CMKCNi(II)-IIP composite adsorbent for Ni(II) ions was 2.44 mg/g adsorbent, the adsorption capacity of the NIP comparator material for Ni(II) ions was 1.65 mg/g adsorbent. The adsorption selectivity was compared to the adsorption ability of Pb(II) ions, the adsorption ability of the adsorbent to Ni(II) ions in samples containing Ni(II) ions, Pb(II) ions and a mixture of Ni(II) and Pb(II) ions, higher than the adsorption capacity of Pb(II).

Conflicts of Interest

The authors declares that there is no conflict of interest regarding the publication of this paper.

Acknowledge

This work was financially supported by Non-APBN Universitas Negeri Malang Fund in 2022 for research grant funding.

References

[1] I. Said. (2022). Nickel pollution pathways in small ecosystem, Egypt. *Arab. J. Geosci.*, *15*(10).
[2] S. Vellaichamy. (2017). Adsorptive separation of copper, nickel, lead, zinc and cadmium from aqueous solution using MWCNTs impregnated with D2EHPA and prior to their determination by FAAS: Kinetic and equilibrium studies. *Sep. Sci. Technol.*, *52*(4), 644-656.
[3] I. Hagarová. (2020). Magnetic solid phase extraction as a promising technique for fast separation of metallic nanoparticles and their ionic species: A review of recent advances. *J. Anal. Methods Chem.*, 2020.

[4] E. Kazemi, A. M. Haji Shabani, and S. Dadfarnia. (2015). Synthesis and characterization of a nanomagnetic ion imprinted polymer for selective extraction of silver ions from aqueous samples. *Microchim. Acta*, *182*(5-6), 1025-1033.

[5] Z. Xie, Y. Chen, L. Zhang, and X. Hu. (2020). Magnetic molecularly imprinted polymer combined with high performance liquid chromatography for selective extraction and determination of the metabolic content of quercetin in rat plasma. *J. Biomater. Sci. Polym. Ed.*, *31*(1), 53-71.

[6] C. Liu, S. Wu, Y. Yan, Y. Dong, X. Shen, and C. Huang. (2019). Application of magnetic particles in forensic science.*TrAC - Trends in Analytical Chemistry*, 121. Elsevier.

[7] M. Yu, L. Wang, L. Hu, Y. Li, D. Luo, and S. Mei. (2019). Recent applications of magnetic composites as extraction adsorbents for determination of environmental pollutants. *TrAC - Trends in Analytical Chemistry*, 119. Elsevier.

[8] Y. Wu *et al.* (2020). Enrichment and sensitive determination of phthalate esters in environmental water samples: A novel approach of MSPE-HPLC based on PAMAM dendrimers-functionalized magnetic-nanoparticles. *Talanta*, 206.

[9] S. Liu *et al.* (2019). Magnetic nanoparticle of metal-organic framework with core-shell structure as an adsorbent for magnetic solid phase extraction of non-steroidal anti-inflammatory drugs. *Talanta*, *194*, 514-521.

[10] Y. Zhang *et al.* (2019). Recent advances in emerging nanomaterials based food sample pretreatment methods for food safety screening. *TrAC - Trends in Analytical Chemistry*, 121. Elsevier.

[11] H. L. Jiang, N. Li, L. Cui, X. Wang, and R. S. Zhao. (2019). "Recent application of magnetic solid phase extraction for food safety analysis. *TrAC - Trends in Analytical Chemistry*, 120. Elsevier.

[12] I. Hagarová. (2020). Magnetic solid phase extraction as a promising technique for fast separation of metallic nanoparticles and their ionic species: A review of recent advances. *J. Anal. Methods Chem.*, 2020.

[13] Y. P. Yew *et al.* (2020). Green biosynthesis of superparamagnetic magnetite Fe_3O_4 nanoparticles and biomedical applications in targeted anticancer drug delivery system: A review. *Arabian Journal of Chemistry*, *13*(1), 2287-2308,

[14] E. Aghaei, R. D. Alorro, A. N. Encila, and K. Yoo. (2017). Magnetic adsorbents for the recovery of precious metals from leach solutions and wastewater. *Metals (Basel).*, *7*(12), 1-32.

[15] R. Nostia, I. K. Kusumaningrum, A. R. Wijaya, B. Zuhroti, and F. Kurniawan. (2020). The capability of nanomagnetite carboxymethyl kappa-carrageenan coated to adsorp metal ions. *AIP Conf. Proc.*, 2215.

[16] L. Y. C. Madruga, R. M. Sabino, E. C. G. Santos, K. C. Popat, R. de C. Balaban, and M. J. Kipper. (2020). Carboxymethyl-kappa-carrageenan: A study of biocompatibility, antioxidant and antibacterial activities. *Int. J. Biol. Macromol.*, *152*, 483-491.

[17] N. N. Purnama *et al.* (2020). Preliminary study on the development of preconcentration method of Cu(II), Co(II), Ni(II), and Cr(III) ions in water samples using nanomagnetite coated by carboxymethyl Kappa-Carrageenan (CMKC). *IOP Conf. Ser. Mater. Sci. Eng.*, 833(1).

[18] D. F. Pratiwi. (2020). Sintesis nanomagnetit karboksimetil kappakaragenan (CMKC) serta aplikasinya sebagai media prekonsentrasi campuran ion logam Ni(II) dan Cr(III) dalam sampel air dengan teknik adsorpsi-desorpsi. Universitas Negeri Malang, 2020.

[19] R. A. Ayuningtyas, I. K. Kusumaningrum, Y. Utomo, Munzil, R. C. Setiawan, A. R. Wijaya, and S. Wonorahardjo. (2021). Synthesis of carboxymethyl kappa -Carrageenan coated nanomagnetite and its application as preconcentration medium for water samples containing Pb(II)-Cu(II) and Pb(II)-Co(II). *AIP Conf. Proc.*, *2330*(II).

[20] R. Nostia. (2019). Kemampuan nanopartikel magnetit terlapis karboksimetil kappa-karagenan untuk mengadsorpsi ion kromium(III) dan nikel(II) pada variasi derajat keasaman (pH) dan waktu kontak adsorpsi. Universitas Negeri Malang.

[21] S. Hidayati, I. K. Kusumaningrum, F. Fajaroh, and A. R. Wijaya. (2021). Development of CMKC-coated nanomagnetite as adsorbent for Pb^{2+} and Cr^{3+} preconcentration process. *AIP Conference Proceedings*, 2353.

[22] L. Y. C. Madruga, R. C. Balaban, K. C. Popat, and M. J. Kipper. (2021). Biocompatible crosslinked nanofibers of poly(vinyl alcohol)/carboxymethyl-Kappa-Carrageenan produced by a green process. *Macromol. Biosci.*, *21*(1), 1-12.

[23] E. O. Ningrum, A. Purwanto, G. C. Rosita, A. Bagus, and T. Suharto. (2017). Konsentrasi cross-linker terhadap performa adsorben berbasis thermosensitive nipam- co -dmaaps gel crosslinker concentration on the performance of the thermosensitive-based adsorbent of nipam-co-dmaaps gel. *J. Tek. Kim. USU*, *12*(1), 9-13.

[24] Z. Zhou *et al.* (2018). Preparation and adsorption characteristics of an ion-imprinted polymer for fast removal of Ni(II) ions from aqueous solution. *J. Hazard. Mater.*, *341*, 355-364.

[25] V. V. Kusumkar, M. Galamboš, E. Viglašová, M. Daňo, and J. Šmelková. (2021). Ion-Imprinted polymers: Synthesis, Characterization, and adsorption of radionuclides. *Materials (Basel).*, *14*(5), 1083.

[26] A. Masykur, S. J. Santosa, D. Siswanta, and Jumina. (2014). Synthesis of Pb(II) imprinted carboxymethyl chitosan and the application as sorbent for Pb(II) ion. *Indones. J. Chem.*, *14*(2), 152-159.
[27] M. Yasinzai *et al.* (2018). Ion-imprinted polymer-based receptors for sensitive and selective detection of mercury ions in aqueous environment. *J. Sensors*, 2018, 1-6.
[28] A. M. Mazrouaa, M. G. Mohamed, and M. Fekry. (2019). Physical and magnetic properties of iron oxide nanoparticles with a different molar ratio of ferrous and ferric. *Egypt. J. Pet.*, *28*(2), 165-171.
[29] S. S. Alterary and A. Alkhamees. (2021). Synthesis, surface modification, and characterization of Fe_3O_4@SiO_2 core@shell nanostructure. *Green Process. Synth.*, *10*(1), 384-391.
[30] A. Alangari *et al.* (2022). Iron oxide nanoparticles: Preparation, characterization, and assessment of antimicrobial and anticancer activity. *Adsorpt. Sci. Technol.*, 2022.
[31] K. Parajuli, A. K. Sah, and H. Paudyal. (2020). Green synthesis of magnetite nanoparticles using aqueous leaves extracts of azadirachta indica and its application for the removal of as(v) from water. *Green Sustain. Chem.*, *10*(04), 117-132.
[32] E. Bertolucci *et al.* (2015). Chemical and magnetic properties characterization of magnetic nanoparticles. *Conf. Rec. - IEEE Instrum. Meas. Technol. Conf.*, 2015, 1492-1496.
[33] R. Salam, A. Dimyati, M. Mujamilah, and M. Silalahi. (2018). Study of magnetic properties of sintered alloy Fe-Cr ODS using VSM. *Journal of Physics: Conference Series*, *1091*(1).
[34] K. Chie, M. Fujiwara, Y. Fujiwara, and Y. Tanimoto. (2003). Magnetic separation of metal ions. *J. Phys. Chem. B*, *107*(51), 14374-14377.
[35] L. Fan *et al.* (2011). Synthesis, characterization and properties of carboxymethyl kappa carrageenan. *Carbohydr. Polym.*, *86*(3), 1167-1174.
[36] I. K. Kusumaningrum, A. R. Wijaya, S. Marfuah, and M. N Fadilah. (2019). Optimation of alkoxide formed step on carboxymethyl Kappa Carrageenan synthesis. *IOP Conf. Ser. Earth Environ. Sci.*, *299*(1), 012008.
[37] S. Ilanlou, M. Khakbiz, G. Amoabediny, J. Mohammadi, and H. Rabbani. (2019). Carboxymethyl kappa carrageenan-modified decellularized small-diameter vascular grafts improving thromboresistance properties. *J. Biomed. Mater. Res. - Part A*, *107*(8), 1690-1701.
[38] J. W. Y. Liew, K. S. Loh, A. Ahmad, K. L. Lim, and W. R. Wan Daud. (2017). Synthesis and characterization of modified κ-carrageenan for enhanced proton conductivity as polymer electrolyte membrane. *PLoS One*, *12*(9), 1-15.
[39] Helmiyati and Y. Anggraini. (2019). Nanocomposites comprising cellulose and nanomagnetite as heterogeneous catalysts for the synthesis of biodiesel from oleic acid. *Int. J. Technol.*, *10*(4), 798-807.
[40] K. Bialik-Wąs, E. Królicka, and D. Malina. (2021). Impact of the type of crosslinking agents on the properties of modified sodium alginate/poly(Vinyl alcohol) hydrogels. *Molecules*, *26*(8), 7-10.
[41] N. F. Yusof, F. S. Mehamod, and F. B. Mohd Suah. (2019). Fabrication and binding characterization of ion imprinted polymers for highly selective Co2+ ions in an aqueous medium. *J. Environ. Chem. Eng.*, *7*(2), 103007.
[42] A. A. Gahlan, S. Hosny, A. Fathi, and O. A. Fargaly. (2023). Removal of Zn, Pb, and Ni heavy metals from aqueous system using efficient modified-banana peel adsorbent. *Curr. Chem. Lett.*, *12*(1), 45-54.